

Resilience of Urban Rail Transit Networks under Compound Natural and Opportunistic Failures

Jack R. Watson^{1,2}, Samrat Chatterjee^{1,2}, *SM-IEEE*, Auroop Ganguly^{2,1}, *SM-IEEE*

¹Pacific Northwest National Laboratory, Richland WA 99352 USA

²Northeastern University, Boston MA 02115 USA

Abstract—Critical infrastructure systems are increasingly at risk of failure due to extreme weather, exacerbated by climate change, and cyber-physical attack, due to reliance on digital information technology. When assessing the state of current infrastructure systems, and when planning new infrastructures, considerations of operational efficiency and resource constraints must be balanced with resilience. A resilient infrastructure design paradigm must account for low-probability, high-impact “grey swan” hazards, and resilience must be structurally embedded by design. This work extends the state-of-the-art in quantification of infrastructure resilience with compound natural-human hazard scenarios and focuses on urban rail transit networks as a proof-of-concept infrastructure system. With new and existing rail projects receiving funding opportunities, an imperative emerges to develop methodological frameworks which can address uncertainty and build resilience into design decisions in addition to operational efficiency. The contributions of this paper are threefold: (1) developing an analytical modeling framework for the simulation of compound failure and recovery in spatially-constrained rail transit networks leveraging system-level awareness; (2) characterizing the dynamics of an urban rail transit network by constructing resilience curves using the largest connected component of the network as a proxy measure for system functionality; and (3) leveraging network science and engineering principles to generate decision-support insights under uncertainty.

Index Terms—Resilience, Rail infrastructure, Network science, Compound hazards.

I. INTRODUCTION & BACKGROUND

A recent study [1] by the President’s National Infrastructure Advisory Council discusses the cyber-physical infrastructure system threat space and exacerbating weather extremes, and indicates the concern associated with a “sophisticated cyber-physical attack resulting in severe physical infrastructure damage; attacks timed to follow and exacerbate a major natural disaster.” The World Economic Forum’s Global Risk Report [2] includes risks with high likelihood and impact as extreme weather events and natural disasters, cyberattacks, and failure of climate change adaptation and mitigation. Consequently, when assessing the state of current critical infrastructure systems, and when planning new infrastructures, considerations of operational efficiency and resource constraints must be balanced with resilience—defined by the U.S. National Academy of Sciences as “the ability to prepare and plan for, absorb, recover from and more successfully adapt to adverse events.” [3] A resilient infrastructure design paradigm must account for low-probability, high-impact grey swan hazards, and resilience must be structurally embedded by design. Typically, the network topology of engineered systems tends to be

constrained by resource limitations and considerations of operational efficiency. As the state of risk and resilience literature evolves, it is increasingly apparent that operational efficiency considerations have tradeoffs in resilience to disruptions [4]. For example, increased connectivity of transit infrastructure may also present failure possibilities via compound natural and opportunistic means that may occur sequentially or simultaneously. There is a need for developing quantitative methods for transit infrastructure resilience against compound hazards that can aid in decision-making during the maintenance and mitigation of current systems and construction of new ones.

As critical infrastructures become more reliant on digital information technology, infrastructure networks become more strongly coupled and interdependent with one another, increasing the possibility of cascading failure within and across networks [5], [6]. What follows is a twofold imperative to plan for resilient-by-design physical and digital infrastructure: first, to structure system topology to be more resilient to increasingly intense, frequent, and hard-to-predict threats, and second, to reconceptualize how critical infrastructure systems are characterized, going beyond low-dimensional, few-component models towards a network-of-networks paradigm more suitable to model interdependencies, feedbacks, and cascading failures between and throughout infrastructures.

This paper contends with two broad modes of failure. The first are those induced by natural hazards, encompassing inundation and physical damage induced by extreme precipitation, storm surge, and high winds. This semi-random failure is expressed as a function of geography, topology, and component-level resilience. The second is targeted failure representing adversarial attack, employing strategic determination of failure sequence so as to maximize loss of system functionality. The latter is in reality bounded by some resource constraints on the part of the adversary, while the former is bounded by physical and statistical assumptions and parameterizations embedded in a given natural hazard model. Recent approaches to modeling natural hazards include Spatially Localized Failure models to simulate typhoon damage on both unimodal and multimodal transportation networks [7]; the development of time-based criticality metrics to capture failure propagation in interdependent transit networks and electrical grids [8]; the use of flood risk models and Coastal Flood Exceedance Probabilities to model potential current and future coastal inundation scenarios [9]; and the use of information from historical events to empirically model the damage to transportation infrastructure resultant from earthquakes [10] and blizzards [11].

The recovery of a damaged rapid transit network can be expressed as a restoration sequence of failed components executed over time. To optimize restoration sequence two sub-problems must be contended with: (1) a metric of instantaneous, time-dependent system functionality must be defined, expressed as a function of network topology, origin-destination traffic flow, or a combination of both; and (2) an algorithmic approach must be developed which determines component recovery sequence while optimizing for minimal loss of system functionality. For a network with N failed components (nodes and/or links) there are $N!$ possible recovery sequences in the solution space and $2^N - 1$ possible intermediate network states. It follows that efficient estimation of optimal recovery sequence is non-trivial and of paramount importance.

The ways in which resilience has been expressed in a rail transport context are numerous, but all rely on the use of quantitative proxies of overall system functionality in the absence of perfect information using system representations with simplifying assumptions. The same holds for damage mitigation during the disruption phase and subsequent determination of recovery sequence: while the methods are numerous, the objective is minimization of cumulative loss of system functionality over the course of the disruption.

Recent work has made progress toward modeling infrastructure networks, and network-of-networks, under individual and compound threat scenarios [12], [13], resilience quantification in complex networks [14], the relationship between topology, dynamics, and resilience [15], defender-attacker models of cyber-physical threat [16], and failure percolation in isolated and interdependent networks [5], [17].

Other recent advancements involve more granular and dynamic considerations of passenger flow within a transit network, integrating both topological and network flow approaches to resilience. Two promising angles of approach are mixed-integer linear programming frameworks in the form of two-stage optimization problems, estimating optimal commuter flows with contingency routing under a variety of failure scenarios [18], [19], and new performance metrics such as “demand impedance” indicators to account for both network structure and passenger travel demand via modified “effective path betweenness” node centrality [20]. Applied case studies have analyzed the system-level resilience of existing rail transit networks subject to disruption [6], [9], [11], [12], [21], but the quantification of resilience, construction of resilience curves accounting for both failure and recovery, and the emphasis on compound natural-human hazard scenarios remain challenging areas of research.

Regardless of the chosen metric of system functionality, failure and recovery dynamics can be expressed as a resilience curve displaying system functionality over time. Overall functionality can be expressed as the integral of such a resilience curve, with baseline normative functionality determined as a (somewhat subjective) “normal” operational functionality integrated over the same span of time. Resilience to a given failure scenario can then be expressed as a scalar parameter representing degradation in functionality during

failure and recovery relative to normal operational function. This enables direct comparison of different failure scenarios and recovery strategies in terms of resilience. It also allows for the comparison of resilience between different real and hypothetical network structures, highly relevant to the planning of new infrastructure systems and of new components in extant systems, a necessary precondition for the structural embedding of resilience-by-design.

This work extends the state-of-the-art and focuses on urban rail transit networks as a proof-of-concept infrastructure system. Rail transport is listed as part of the national critical function set by the Cybersecurity and Infrastructure Security Agency (CISA) of the U.S. Department of Homeland Security (DHS) [22]. With new and existing rail projects receiving funding opportunities, an imperative emerges to develop methodological frameworks which can address uncertainty and build resilience into design decisions in addition to operational efficiency. The contributions of this paper are threefold: (1) developing an analytical modeling framework for the simulation of compound failure and recovery in spatially-constrained rail transit networks leveraging system-level awareness; (2) characterizing the dynamics of an urban rail transit network by constructing resilience curves using the largest connected component of the network as a proxy measure of system functionality; and (3) leveraging network science and engineering principles to generate decision-support insights under uncertainty.

The remainder of this paper is organized as follows. Section 2 describes the methodological framework for simulating failure and recovery of rail networks under compound natural and opportunistic hazards, including network science-derived algorithmic approaches. Section 3 presents the numerical simulation case study in an urban rail transit network environment. Section 4 presents and discusses preliminary results. Section 5 offers concluding remarks and steps for future research.

II. METHODOLOGY

Based on the definition of resilience by the U.S. National Academy of Sciences with phases of plan, absorb, recover, and adapt [3], [14], we first conceptualize compound natural and opportunistic failures as sequential disruptions. In the sequential case, the perturbed network may not have recovered to full functionality before experiencing a second disruption, as presented in Figure 1. Here compound failure occurs when a first failure event or disruption results in a reduction of system functionality followed by a second disruption before the system begins recovering from the first. The recovery phase includes post-disaster response and repairs. The dotted line in the adaptation phase represents the potential to learn and adapt from past disruptions to increase resilience to possible future hazards.

To quantify resilience as a function of system functionality in the discrete-time case we sum instantaneous system functionality over the extent of the failure and recovery period, normalized as a fraction of a normative baseline functionality over the same number of discrete time steps. [23] Let $\psi(t)$ be

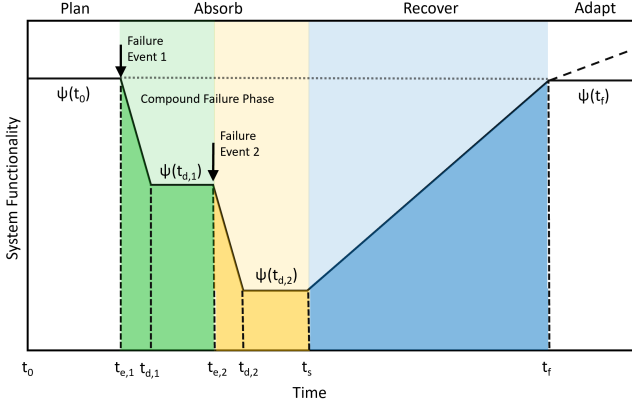


Fig. 1: Infrastructure system resilience phases. t_0 marks the start of the window of interest in the planning phase. $t_{e,i}, t_{d,i}$ denote the commencement and conclusion of a disruption event, encompassing the absorption phase. t_s, t_f denote the start and finish of the recovery phase. $\psi(t)$ gives a measure of instantaneous system functionality. The green and yellow shaded boxes indicate the first and second sequential disruption events, and blue the recovery phase. White indicates some normal state of operation corresponding to the planning and adaptation phases. The darkened area under the curves represents the integral of system performance over time. The dashed horizontal line from t_0 to t_f indicates normal system performance over the same window of time.

a measure of instantaneous system functionality at time t . In accordance with figure 1, let $\psi(t_0)$ and $\psi(t_f)$ be the initial pre-disruption system functionality and final, post-recovery system functionality. Let $(t_{e,i}, t_{d,i})$ represent the start and end times of sequential disruption i . We assume that full recovery is achievable, i.e., $\psi(t_0) = \psi(t_f)$. Lastly, let t_s be the time at which recovery begins.

$E = \{e_1, \dots, e_i\}$ represents the set of disruptions to which the system is subjected, proceeding sequentially from e_1 . In the scenario described in the next section, $E = \{e_1, e_2\}$ represents sequential natural and targeted disruptions. Recovery strategy is a function of C_ρ , denoting the measure with which component importance is evaluated to determine recovery sequence.

We initially assume that system functionality is a function of topology, without loss of generality. $\psi(t)$ is determined by G_t , which is in turn a function of G_{t-1} and either e_i or C_ρ depending on the phase. This can be expressed as $\psi(t) \sim f(G_{t-1}, E, C_\rho)$ where f is some function that returns a measure of system functionality. Graph state G_t is a function of previous system state G_{t-1} , disruption events E , and recovery strategy C_ρ . Time is implicit, and the number of time steps $t \in T$ before halting is a function of the number of vertices in the initial graph state G_0 . Letting $\psi(t_0)$ be the normative baseline system functionality, resilience can be

quantitatively defined and measured as:

$$R(G|E, C_\rho) = \frac{\sum_{t \in \{t_{e,1}, \dots, t_f\}} \psi(t)}{\psi(t_0)(t_f - t_{e,1})} \quad (1)$$

That is, the resilience of the system is the area under the curve across the time frame of interest divided by the area under normal functionality over the same span of time. The evolution of the system depends on the previous graph state and the phase of the system:

$$\psi(t) \sim f(G_t) = \begin{cases} f(G_{t-1}, e_n), & \text{if } t_{e,n} \leq t < t_{e,n+1}, \\ f(G_{t-1}, e_i), & \text{if } t_{e,i} \leq t < t_s, \\ f(G_{t-1}, C_\rho), & \text{if } t_s \leq t \leq t_f. \end{cases} \quad (2)$$

Resilience values close to 1 indicate an effective absorption of and recovery from disruptions (the system is resilient), while values close to 0 indicate a failure to absorb and recover from disruptions (the system is not resilient). Expressing resilience as a scalar ratio enables direct comparison of the efficacy of multiple targeting and recovery strategies.

The number of operational nodes contained within a network's giant (or largest) connected component (GCC) is used as a static topological proxy for system functionality [24]. The GCC is the largest subgraph of a network from which every node in the subgraph is reachable by every other node in the subgraph. We use several metrics of network centrality to define exploitation and recovery strategies. Network centrality measures assign a weight of relative importance to each node or edge in a graph as a function of network position. Nodes that are more central are assigned higher centrality scores. In equations (1) and (2), C_ρ can take the form of any of the preceding centrality measures. Of particular interest is betweenness centrality; the betweenness centrality of a node is the number of shortest paths in a graph that contain the node, but for which that node is not an endpoint. Betweenness centrality has been shown to outperform optimization-based greedy algorithms, and match the performance of cross-entropy approaches, in the approximation of optimal network recovery sequence when applied to existing rail transit networks [11]. Other applicable centrality measures include eigenvector, closeness, and Katz centrality.

Here we describe the formulation of degree, closeness, eigenvector, and betweenness centrality, the four network centrality measures explored for targeting and recovery sequence determination. For a given undirected graph $G = (V, E)$ with V vertices (nodes) and E edges (links), vertex-level degree centrality $C_D(v)$ is simply the count of edges connecting to a given vertex, [25] or:

$$C_D(v) = \deg(v) \quad (3)$$

Closeness centrality is the normalized average network distance of the shortest path from vertex v to all other vertices u . [26] Closeness is undefined for a graph that is not weakly connected and is useful within our framework because any state during numerical simulation considers only the giant connected component of the graph. If we let $d(u, v)$ represent

the shortest path between vertices u and v , then for a graph with V vertices, normalized closeness centrality is expressed as:

$$C_C(v) = \frac{V-1}{\sum_u d(u,v)} \quad (4)$$

Eigenvector centrality defines a vertex-level measure of relative importance by scoring vertices based on the eigenvector centrality of their immediate neighbors in a graph. [27] Intuitively, this means that influence is determined by how connected one is to others who hold great influence. Mathematically, letting $A = (a_{v,u})$ be the adjacency matrix of graph $G = (V, E)$ and λ a constant, this can be expressed in vector notation as the eigenvector equation $Ax = \lambda x$. If we choose to represent this in scalar notation, letting $M(v)$ be the set of vertices neighboring vertex v , eigenvector centrality becomes:

$$C_E(v) = \frac{1}{\lambda} \sum_{u \in M(v)} C_E(u) = \frac{1}{\lambda} \sum_{u \in V} a_{v,u} C_E(u) \quad (5)$$

Lastly, betweenness centrality describes the normalized fraction of all shortest paths in a graph that traverse a given vertex v , but for which v is not an endpoint itself. [28] Betweenness centrality is useful for identifying components that bridge disparate communities in a graph, or viewed alternatively, components that act as bottlenecks for information or commodities (or trains) circulating through a network. For this reason betweenness centrality is an attractive proxy for network flow in the absence of such dynamics. Letting $\sigma_{s,t}$ be the number of shortest paths between vertices s and t (typically $\sigma_{s,t} = 1$ unless multiple equidistant paths exist), and letting $\sigma_{s,t}(v)$ be the number of paths in $\sigma_{s,t}$ that contain vertex v , betweenness centrality can be expressed as:

$$C_B(v) = \sum_{s \neq v \neq t \in V} \frac{\sigma_{s,t}(v)}{\sigma_{s,t}} \quad (6)$$

Figure 2 presents our methodological workflow including data, algorithms, and simulation components. Rail network topology, geographical information, flood maps, and network science methodology are combined to simulate compound failure (i.e., flooding followed by opportunistic exploitation) and subsequent recovery of a transit system. Loss of system functionality due to a hypothetical flooding (natural) event can be modeled using the output of dynamic flood models or with static flood risk or water level maps. The benefit of the latter is the wide public availability of expert-generated flood map data, which improves the ease of reproducibility. However, this requires stronger assumptions to be made during simulation, namely that rail stations (nodes) falling within inundated areas flood in order of lowest to highest elevation. For the present study, the dimension of time is implicit without inclusion of a dynamical flood model component.

Following the flooding phase of failure, opportunistic failure is induced by calculating centrality measures for each node in the network at each point in time, targeting the component with the highest centrality, then recalculating and repeating

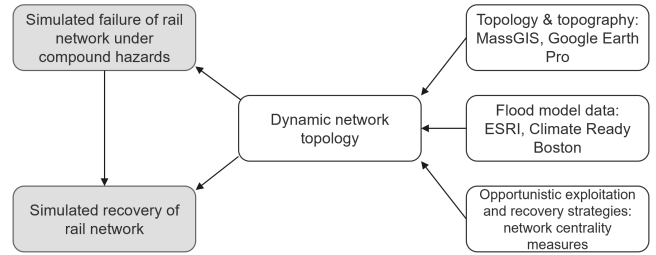


Fig. 2: Methodological workflow.

over time until no nodes remain in the largest connected component. As branches of the system are disconnected from the largest connected component, these smaller disconnected components are considered unreachable indirect failures. In the recovery phase, nodes in the initial intact network are statically sorted by centrality measure, then components are repaired in order of highest to lowest centrality. Betweenness, degree, eigenvector, and closeness centrality were considered for both exploitation and recovery. In this setup compound disruptions are treated as sequential, and it is assumed that an adversary inducing opportunistic failure possesses complete knowledge of the network's topology, opportunistically timing failure following a catastrophic flooding event that has already damaged infrastructure. Algorithm 1 presents pseudocode for compound failure simulations, reflecting sequential flooding and opportunistic exploitation of a rail transit network. Betweenness centrality is shown here as an example of a centrality measure that takes a graph as an input and returns the index of a node to exploit as an output. Algorithm 2 corresponds to recovery of a partially or completely degraded network. The recovery phase leverages the same network centrality measures as does opportunistic failure. However, the algorithmic approach in the recovery phase is not a translation or reflection of our targeted failure phase: the key difference lies in the dynamic, iteratively-updated centrality during failure versus the static, one-shot centrality calculation utilized in recovery. In the next section, we describe the urban rail transit case study to which we apply our methodological framework.

III. NUMERICAL SIMULATION

The Massachusetts Bay Transportation Authority's rapid transit system, known colloquially as "The T", services the city of Boston and surrounding urban-suburban areas with light rail (streetcar) and rapid transit (subway) lines. The T was chosen as an initial proof-of-concept case study as it represents a subgraph of the transit network in the greater Boston-Washington rail transit network-of-networks and serves as a methodological test bed that in the future can be scaled up further to include commuter rail and intercity lines connecting multiple rail systems.

Figure 3 presents the case study region in Boston with the T network structure and the projected 1-in-100-year flood

Algorithm 1 Compound Failure

- 1: $G(N, E)$: graph of transit network with nodes N and edges E
- 2: $n_i \in N$: set of nodes (stations) in G
- 3: G_{GCC} : subgraph of G indicating giant (weakly) connected component
- 4: G' : updated graph subject to failure such that $G = G'(t_0)$
- 5: $s_i \in S$: subset of nodes falling within inundated area
- 6: Sort S in order of ascending elevation
- 7: **for** $s_i \in S$ **do**
- 8: Remove s_i from G'
- 9: Remove edges e_{s_i} connected to s_i from G'
- 10: Recalculate G'_{GCC}
- 11: **end for**
- 12: Let $G' = G'_{GCC}$ to account for indirect failure
- 13: **for** $i = 1, 2, \dots, N \in G'(N, E)$ **do**
- 14: Initialize $n_{C_{max}} = 0$
- 15: **for** $n_i \in N$ **do**
- 16: $C(n_i) = \sum_{s \neq n_i \neq t} \frac{\sigma_{st}(n_i)}{\sigma_{st}}$
- 17: **if** $C(n_i) > n_{C_{max}}$ **then**
- 18: $n_{C_{max}} = C(n_i)$
- 19: **end if**
- 20: **end for**
- 21: Remove $n_{C_{max}}$ from G'
- 22: Remove $e_{C_{max}}$ from G'
- 23: Recalculate G'_{GCC}

Algorithm 2 Recovery

- 1: G' : initially empty graph subject to recovery such that $G'(t_0) = 0$ and $G'(t_N) = G$
- 2: **for** $n_i \in G(N, E)$ **do**
- 3: $C(n_i) = \sum_{s \neq n_i \neq t} \frac{\sigma_{st}(n_i)}{\sigma_{st}}$
- 4: **end for**
- 5: Let $C(G)$ be the vector of all centrality scores calculated in (3.)
- 6: Initialize $G'_{GCC} = 0$, the giant connected component of G'
- 7: **for** $n_i \in G(N, E)$ **do**
- 8: Let $n_{C_{max}} = \max(C(G))$
- 9: Remove $n_{C_{max}}$ from $C(G)$
- 10: Add $n_{C_{max}}$ to G'
- 11: **if** edges exist between nodes in G that exist in G' **then**
- 12: Add edges to G'
- 13: **end if**
- 14: Update G'_{GCC}

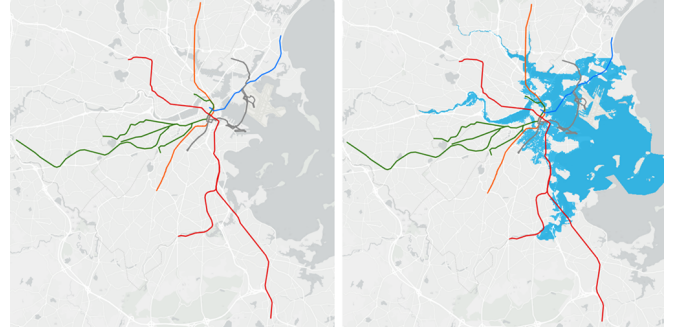


Fig. 3: Proof-of-concept case study region. (Left) the network structure of the T with colors (orange, red, blue, green, and silver) corresponding to various network lines, the Massachusetts Bay Transportation Authority’s rapid transit and light rail system serving metropolitan Boston, MA. (Right) the T overlaid with an inundation map of a projected 1-in-100-year flood on top of a 3-foot mean sea level rise baseline.

map. Data sources consist of publicly available datasets from government agencies and crowd-sourced repositories. We use a projected 1-in-100-year flood map with a baseline 3 feet of sea level rise to represent possible future extreme hazard conditions [29]. This scenario represents a pessimistic (RCP 8.5) emissions trajectory around year 2100 [30]. The T is linear and branching, like a dendrogram in network structure. There is little redundancy in the network, and six central nodes connect the four subway lines in downtown Boston. All six of the critical nodes connecting the lines of the T together occupy a relatively small, dense area in Boston’s downtown, proximal to the coastline and to each other.

IV. RESULTS AND DISCUSSION

Preliminary results include identification of key rail stations (nodes) inundated under a 1-in-100-year flooding scenario on top of 36” baseline sea level rise, resulting in fragmentation of network topology following the nonoperational assumption of inundated stations. Figure 4 identifies flood-prone stations on the orange, red, and blue lines that disconnect northern, southern, and eastern subway lines from the network’s giant connected component.

Initial simulation results take the form of resilience curves. Figure 5 presents a scenario of catastrophic flooding followed sequentially by opportunistic exploitation. To simulate strategic targeted failure during the opportunistic exploitation phase, we employ network centrality measures to determine failure sequence. Performance is then compared to an averaging of randomly-determined node exploitation sequences. Following failure, the recovery phase is simulated using the same suite of centrality measures embedded in a different algorithmic procedure. Likewise, the performance of an ensemble mean of randomly-selected node recovery sequences is used as a baseline. In Figure 5, closeness-based opportunistic exploitation following flooding-induced failure leads to maximal degrada-

tion of functionality as defined by GCC size. Betweenness centrality performs nearly as effectively, with a resilience measure 0.82% greater than closeness. In all cases explored herein, network centrality-based failure strategies lead to more severe loss of functionality than random failure strategy (determined as the mean of 500 random failure simulation runs), and the majority of targeted failure curves fall outside the bounds of the 95% confidence interval of random failure. Figure 6 shows the step-by-step fragmentation of the T during flooding and betweenness-targeted failure.

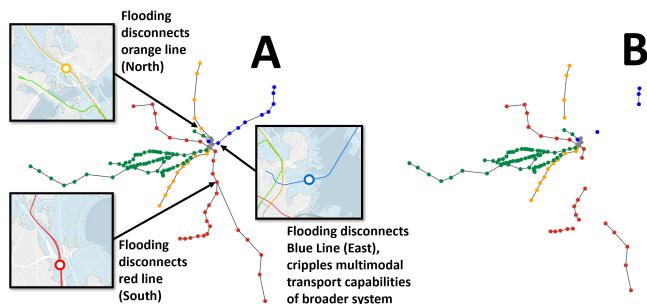


Fig. 4: (A) Network topology of the T with three key stations on different subway lines inundated under 1-in-100-year flooding scenario. (B) Fragmented network topology of the T following functionality loss of inundated stations.

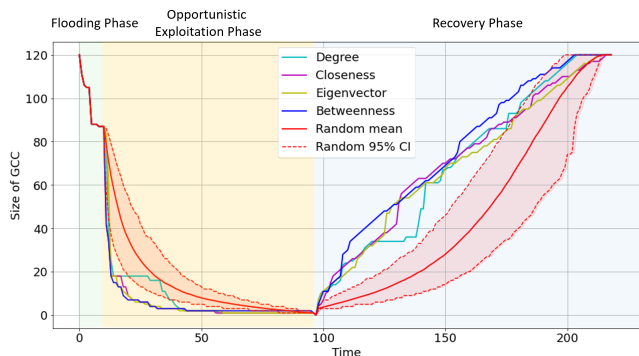


Fig. 5: Resilience curve showing compound failure and recovery profiles from numerical simulations.

The recovery phase begins assuming zero system functionality with all nodes in the network disabled. Figure 4 shows the centrality-based recovery approach employed, and the right half of Figure 5 (blue) shows the relative performance of different centrality measures compared to a random baseline. All centrality-based recovery strategies outperform random recovery and exceed the 95% confidence interval. Betweenness centrality demonstrates performance closest to an optimal strategy, maximizing the integral of system functionality (area under the curve) compared to degree, closeness, and eigenvector centrality.

To determine the most and least optimal strategies for disruption and recovery, permutations of strategies for each phase were produced. Table I presents resilience measures

for all combinations of strategies considered in this study. As can be gleaned intuitively from figure 5, the most resilient combination of strategies are the case in which the disruption strategy is entirely random, while the recovery strategy uses betweenness. The least resilient scenario is that in which flooding disruption is followed by closeness-based targeted disruption and recovery is unintelligent and purely random. Table I presents best-performing strategy combinations in green and worst-performing strategy combinations in red. Across the board, strategic recovery strategies outperform random recovery sequence in maintaining system functionality. The exception is the upper 95% confidence bound of the random ensemble; to approach the performance of intelligent strategy, random recovery must by chance determine a component repair sequence that approximates the results of centrality measure-based recovery, a highly unlikely occurrence. Of additional emphasis is the strikingly poor performance of the lower 5% confidence interval of the random ensemble for recovery in combination with all failure strategies, indicating that when recovery sequence is far from optimal, the ability to absorb a disruption is dominated by the inability to recover from it, and the resultant performance loss is substantial.

While the same set of centrality measures are utilized in both failure and recovery routines, failure and recovery are not symmetrical mirror-images of one another as is observed in the random ensemble. This serves to emphasize the need for researchers, stakeholders, and policymakers to consider both failure and recovery dynamics of networked infrastructure systems across a range of environmental scenarios when modeling such systems and translating findings to policy decisions. It is also worth noting that the MBTA network is here being modeled as an isolated network with no interdependencies between rail transit, power, communication, and multimodal transportation networks. This simplifying assumption allows for resilience quantification, but does not reflect the possibility of cascading failures between interdependent systems. Rail transit requires a functioning electrical grid and reliable communication network to operate, and functional road transportation is required for physical repair during recovery.

Resilience curves such as those presented here have the potential to inform what-if scenario analyses and generate insights for stakeholder decision-making regarding operation, planning, mitigation, and adaptation of urban rail transit networks subject to compound failures. Our simulation framework is adaptable to a broad range of potential failure and recovery scenarios and was designed to be extensible to other types of infrastructure networks, both in isolation and integrated together as a network-of-networks. In future work, two aspects of infrastructure resilience are of primary focus: one is the integration of multiple scales of infrastructure, such as urban, regional, and inter-city transit, within a unified simulation framework. The second is the integration of multiple qualitative, interdependent lifeline networks, motivated by the potential for cascading failure between systems.

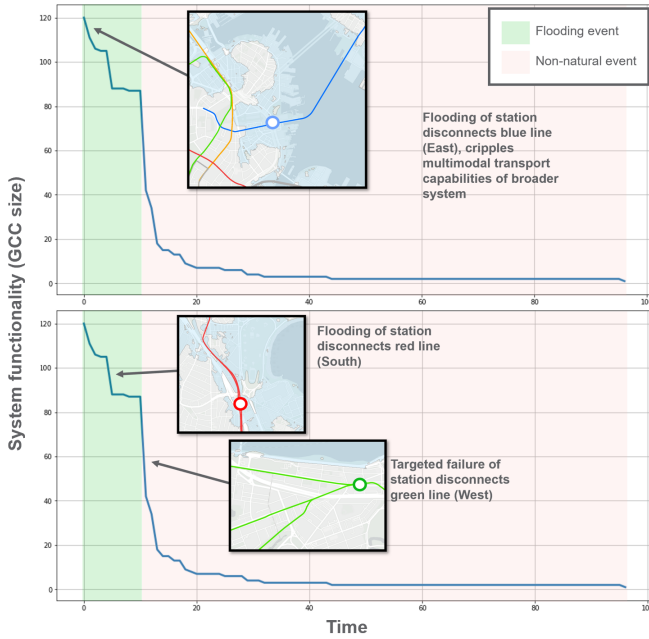


Fig. 6: Top: in our simulation of Boston’s T urban rail network, the first station to fail due to inundation is a subterranean coastal station near sea level, isolating Logan International Airport from the rapid transit system. Bottom: the subsequent flooding of a coastal station to the south of Boston disconnects a large portion of the red line. Following the flooding phase of failure, the targeted phase involves failure of a green line station that disconnects the extensive Westward street car network.

V. CONCLUDING REMARKS & FURTHER WORK

The simulation of an urban-scale transit system subject to compound failure and recovery has furthered a primary objective of ongoing research: the simulation of interconnected infrastructure systems on urban, regional, and continental scales. A second priority objective in the future of this project is the generation and simulation of traffic flow dynamics, potentially allowing for the observation of emergent behavior. This is closely related with the objective of including the possibility of partial functionality on a component-level; the simulation presented in this report allows only for binary on/off functionality of train stations, and partial functionality in the form of reduced capacity will allow for the relaxation of such a simplifying assumption. Other areas for improvement include more granular and realistic representation of edges (rail segments), particularly for subterranean subway systems prone to inundation [9], and the development of new and integration of existing measures of resilience that factor in economic damage, as recent work suggests that purely topological quantifications of resilience fail to capture resultant economic impacts [8].

Such dynamic passenger flow approaches are particularly critical given recent work demonstrating that the resilience of transit networks to disruption is highly dependent on the

state of traffic flow at the time of disruption [31]. In the first section of this paper, recent advancements in the application of multi-level optimization to transit networks was discussed; specifically, [18], [19] optimize train scheduling, passenger routing, and bus bridging in order to avoid traffic states that are highly vulnerable to disruption. Combining resilience on the level of passenger flow with compound topology-based metrics of resilience [20] and network operation changes for purposes of planning new infrastructures [32] is imperative for a comprehensive understanding of the resilience and consideration of the modification of existing transit systems, and for planning new transit systems on urban to continental scales.

TABLE I: Overall resilience measures considering compound failure and recovery. The best-performing combination of strategies are shown in green ($R = 0.4645$), and worst in red ($R = 0.2120$).

		Resilience Measure						
		Recovery						
degree		0.3903	0.3805	0.3824	0.3809	0.4122	0.4358	0.3925
closeness		0.3963	0.3865	0.3885	0.3870	0.4182	0.4418	0.3985
eigenvector		0.3892	0.3794	0.3813	0.3798	0.4111	0.4347	0.3914
betweenness		0.4190	0.4092	0.4112	0.4097	0.4409	0.4645	0.4212
random mean		0.2911	0.2813	0.2832	0.2817	0.3130	0.3366	0.2933
	95%	0.3545	0.3447	0.3467	0.3452	0.3764	0.4000	0.3567
	5%	0.2217	0.2120	0.2139	0.2124	0.2437	0.2673	0.2240
	Failure	degree	closeness	eigenvector	betweenness	random mean	95%	5%

The novel contributions here serve as a data pipeline and analytical framework for the modeling and simulation of networked infrastructure systems under compound hazards. Future efforts will include physics-informed hazard dynamics of greater complexity, implementation of partial functionality of disrupted infrastructure components, further development of methods for the quantification of system-wide resilience, and exploration of optimization-based recovery strategies. Consideration of traffic flow in the context of operational efficiency and resilience to disruptions and the expansion of system boundaries to include urban, commuter, and intercity rail transit as an interconnected network-of-networks may also lead to the development of scalable algorithmic methods driven by both data and theory.

VI. ACKNOWLEDGMENTS

This research was partially funded by the DOD SERDP grant # RC20-1183 titled “Networked Infrastructures under Compound Extremes”.

REFERENCES

- [1] N.I.A.C., "Surviving a Catastrophic Power Outage: How to Strengthen the Capabilities of the Nation," National infrastructure advisory board, Tech. Rep., 2018.
- [2] A. Collins, K. Schwab, and R. Samans, "The Global Risks Report 2018," World Economic Forum, Tech. Rep., 2018.
- [3] National Research Council, *Disaster resilience: A national imperative*, 2012.
- [4] A. S. Jin, B. D. Trump, M. Golan, W. Hynes, M. Young, and I. Linkov, "Building resilience will require compromise on efficiency," *Nature Energy*, vol. 6, no. 11, pp. 997–999, 2021.
- [5] S. V. Buldyrev, R. Parshani, G. Paul, H. E. Stanley, and S. Havlin, "Catastrophic cascade of failures in interdependent networks," *Nature*, vol. 464, no. 7291, pp. 1025–1028, 2010.
- [6] R. Twumasi-Boakye and J. Sobanjo, "Civil infrastructure resilience: state-of-the-art on transportation network systems," *Transportmetrica A: Transport Science*, vol. 15, no. 2, pp. 455–484, 2019. [Online]. Available: <https://doi.org/10.1080/23249935.2018.1504832>
- [7] C. Fang, Y. Chu, H. Fu, and Y. Fang, "On the resilience assessment of complementary transportation networks under natural hazards," *Transportation Research Part D: Transport and Environment*, vol. 109, 8 2022.
- [8] X. B. Wee, M. Herrera, G. M. Hadjidemetriou, and A. K. Parlikad, "Simulation and criticality assessment of urban rail and interdependent infrastructure networks," *Transportation Research Record*, vol. 0, no. 0, p. 03611981221103594, 0. [Online]. Available: <https://doi.org/10.1177/03611981221103594>
- [9] M. V. Martello, A. J. Whittle, J. M. Keenan, and F. P. Salvucci, "Evaluation of climate change resilience for Boston's rail rapid transit network," *Transportation Research Part D: Transport and Environment*, vol. 97, no. June, p. 102908, 2021. [Online]. Available: <https://doi.org/10.1016/j.trd.2021.102908>
- [10] M. Aghababaei, S. B. Costello, and P. Ranjitkar, "Transportation impact assessment following a potential alpine fault earthquake in new zealand," *Transportation Research Part D: Transport and Environment*, vol. 87, p. 102511, 2020. [Online]. Available: <https://www.sciencedirect.com/science/article/pii/S1361920920306982>
- [11] U. Bhatia, L. S. Perelman, and A. R. Ganguly, "Generalized network recovery based on topology and optimization for real-world systems," *arXiv*, 2018.
- [12] N. Yadav, S. Chatterjee, and A. R. Ganguly, "Resilience of Urban Transport Network-of-Networks under Intense Flood Hazards Exacerbated by Targeted Attacks," *Scientific Reports*, vol. 10, no. 1, pp. 1–14, 2020. [Online]. Available: <http://dx.doi.org/10.1038/s41598-020-66049-y>
- [13] S. Dong, X. Gao, A. Mostafavi, and J. Gao, "Modest flooding can trigger catastrophic road network collapse due to compound failure," *Communications Earth Environment*, vol. 3, no. 1, pp. 1–10, 2022.
- [14] I. Linkov, T. Bridges, F. Creutzig, J. Decker, C. Fox-Lent, W. Kröger, J. H. Lambert, A. Levermann, B. Montreuil, J. Nathwani, R. Nyer, O. Renn, B. Scharte, A. Scheffler, M. Schreurs, and T. Thiel-Clemen, "Changing the resilience paradigm," *Nature Climate Change*, vol. 4, no. 6, pp. 407–409, 2014. [Online]. Available: <http://dx.doi.org/10.1038/nclimate2227>
- [15] J. Gao, B. Barzel, and A. L. Barabási, "Universal resilience patterns in complex networks," *Nature*, vol. 530, no. 7590, pp. 307–312, 2016.
- [16] M. R. Oster, S. Chatterjee, A. R. Ganguly, D. G. Thomas, J. Watson, D. Corbani, J. Webster, F. Pan, B. Gattis, and K. Haynie, "A Tri-Level Optimization Model for Interdependent Infrastructure Network Resilience Against Compound Hazard Events," *2021 IEEE Virtual IEEE International Symposium on Technologies for Homeland Security, HST 2021*, pp. 2021–2023, 2021.
- [17] S. Panzieri and R. Setola, "Failures propagation in critical interdependent infrastructures," *International Journal of Modelling, Identification and Control*, vol. 3, no. 1, pp. 69–78, 2008.
- [18] L. Xu and T. S. A. Ng, "A robust mixed-integer linear programming model for mitigating rail transit disruptions under uncertainty," *Transportation Science*, vol. 54, no. 5, pp. 1388–1407, 2020. [Online]. Available: <https://doi.org/10.1287/trsc.2020.0998>
- [19] J. Tang, L. Xu, C. Luo, and T. S. A. Ng, "Multi-disruption resilience assessment of rail transit systems with optimized commuter flows," *Reliability Engineering System Safety*, vol. 214, p. 107715, 10 2021.
- [20] J. Chen, J. Liu, Q. Peng, and Y. Yin, "Resilience assessment of an urban rail transit network: A case study of chengdu subway," *Physica A: Statistical Mechanics and its Applications*, vol. 586, p. 126517, 1 2022.
- [21] Y. Saadat, B. M. Ayyub, Y. Zhang, D. Zhang, and H. Huang, "Resilience of Metrorail Networks: Quantification With Washington, DC as a Case Study," *ASCE-ASME J Risk and Uncert in Engrg Sys Part B Mech Engrg*, vol. 5, no. 4, pp. 1–14, 2019.
- [22] CISA, "National Critical Functions Set," pp. 1–3, 2021. [Online]. Available: <https://www.dhs.gov/cisa/national-critical-functions>
- [23] K. Barker, J. E. Ramirez-Marquez, and C. M. Rocco, "Resilience-based network component importance measures," *Reliability Engineering System Safety*, vol. 117, pp. 89–97, 2013. [Online]. Available: <https://www.sciencedirect.com/science/article/pii/S0951832013000823>
- [24] M. Kitsak, A. A. Ganin, D. A. Eisenberg, P. L. Kravivsky, D. Krioukov, D. L. Alderson, and I. Linkov, "Stability of a giant connected component in a complex network," *Physical Review E*, vol. 97, no. 1, pp. 1–7, 2018.
- [25] S. L. Hakimi, "On realizability of a set of integers as degrees of the vertices of a linear graph. i," *Journal of the Society for Industrial and Applied Mathematics*, vol. 10, no. 3, pp. 496–506, 1962. [Online]. Available: <https://doi.org/10.1137/0110037>
- [26] A. Bavelas, "Communication patterns in task-oriented groups," *The Journal of the Acoustical Society of America*, vol. 22, no. 6, pp. 725–730, 1950. [Online]. Available: <https://doi.org/10.1121/1.1906679>
- [27] P. Bonacich, "Some unique properties of eigenvector centrality," *Social Networks*, vol. 29, no. 4, pp. 555–564, 2007. [Online]. Available: <https://www.sciencedirect.com/science/article/pii/S0378873307000342>
- [28] L. C. Freeman, "A set of measures of centrality based on betweenness," *Sociometry*, vol. 40, no. 1, pp. 35–41, 1977. [Online]. Available: <http://www.jstor.org/stable/3033543>
- [29] The Boston Research Advisory Group, "Climate Change and Sea Level Rise Projections for Boston," Climate Ready Boston, Tech. Rep., 2016.
- [30] B. P. Horton, N. S. Khan, N. Cahill, J. S. Lee, T. A. Shaw, A. J. Garner, A. C. Kemp, S. E. Engelhart, and S. Rahmstorf, "Estimating global mean sea-level rise and its uncertainties by 2100 and 2300 from an expert survey," *npj Climate and Atmospheric Science*, vol. 3, no. 1, pp. 1–8, 2020. [Online]. Available: <http://dx.doi.org/10.1038/s41612-020-0121-5>
- [31] N. Bešinović, R. Ferrari Nassar, and C. Szymula, "Resilience assessment of railway networks: Combining infrastructure restoration and transport management," *Reliability Engineering System Safety*, vol. 224, p. 108538, 2022. [Online]. Available: <https://www.sciencedirect.com/science/article/pii/S0951832022001909>
- [32] H. E. Tan, J. H. W. Oon, N. B. Othman, E. F. Legara, C. Monterola, and M. A. Ramli, "Quantifying the resilience of rapid transit systems: A composite index using a demand-weighted complex network model," *PLOS ONE*, vol. 17, p. e0267222, 4 2022. [Online]. Available: <https://journals.plos.org/plosone/article?id=10.1371/journal.pone.0267222>